THE JOURNAL OF NAVIGATION (2003), **56**, 429–441. © The Royal Institute of Navigation
DOI: 10.1017/S037346330300242X Printed in the United Kingdom

Dynamic Localization of Car-like Vehicles using Data Fusion of Redundant ABS Sensors

Ph. Bonnifait, P. Bouron, D. Meizel and P. Crubillé

(*Université de Technologie de Compiègne*, *France*)

A localization system using GPS, ABS sensors and a driving wheel encoder is described and tested through real experiments. A new odometric technique using the four ABS sensors is presented. Due to the redundancy of measurements, the precision is better than the method using differential odometry on the rear wheels only. The sampling is performed when necessary and when a GPS measurement is performed. This implies a noticeable reduction of the GPS latency, simplifying the data-fusion process and improving the quality of its results.

KEY WORDS

1. GPS. 2. Odometry. 3. Data fusion. 4. Kalman filtering.

1. INTRODUCTION. Real-time continuous localization is essential for many applications concerning outdoors vehicles (Guivant, Nebot and Baiker, 2000; Zhao, 2000). It consists of estimating the vehicle location in a global digital map. GPS is a very attractive solution because it is affordable and convenient. Moreover, since May 2000, when the SA degradation was turned off, the precision is sufficient for the usual navigation tasks. Nevertheless, GPS still suffers from an "obscuration of signals" occurring in urban environments, under bridges, in tunnels or forests. When a GPS obscuration occurs, fewer than four *good satellites* are visible and the receiver is not able to compute an estimate of the position. The phrase "*good satellites*" means satellites which present a sufficient elevation angle, a good signal to noise ratio and a good geometrical configuration. GPS appears then as an intermittent positioning system that demands the help of a dead-reckoning system. Commercially available solutions use an odometer, a gyro and sometimes a magnetic compass (Abbott and Powel, 1999) to maintain an estimation of position during the obscuration of GPS signals. In modern cars, braking is assisted by ABS systems that use angular encoders attached to the wheels. In such a case, the sensors basically measure the wheel speeds. We propose in this paper to use this data to estimate the distances travelled and then to implement an odometric technique. Odometry can advantageously replace the commercially available dead-reckoning techniques that use supplementary sensors like gyros (Barshan and Durrant-Whyte, 1995; Chung, Ojeda and Borenstein, 2001). The models presented in this paper are real odometric models and not the discretized kinematics models used in Julier and Durrant-Whyte, 1995. Assumptions are made on the elementary motions and

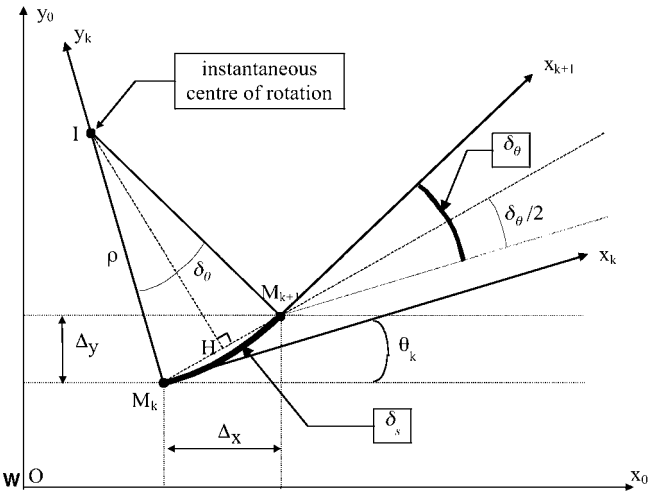

Figure 1. Elementary displacement between 2 samples.

geometric relationships are expressed to provide relations between the rotations of the wheels and the displacements.

The paper is organized as follows. Section two describes an odometric technique using four ABS sensors together with an encoder measuring the driving wheel angle. These measurements are fused via an Extended Kalman Filter. Special attention is dedicated to the sampling process that is customized to the GPS. This is done by taking both the displacement and time as progression variables. Experiments show the efficiency of this technique in comparison with differential odometry using just the rear wheel sensors. The complete localizer is then presented in section three. Experiments performed with a laboratory car quantify the precision obtained when the GPS is available and when GPS obscuration occurs. Section four presents the conclusion.

2. ODOMETRY WITH ABS SENSORS.

The purpose of odometry is to build an incremental model of the vehicle motion using measurements of the basic wheel rotations. Numerous non-linear models are available in the literature (Bétaille and Bonnifait, 2002; Kochem, Wagner, Hamann and Isermann, 2002). In this section, we first introduce the generic integration process whose inputs are theoretical quantities (not directly measured). These inputs are then estimated using the measurements from all the encoders.

2.1. *Integration process.*

The mobile frame **M** of a car-like vehicle is chosen with its origin M attached to the centre of the rear axle. The x-axis is aligned with the longitudinal axis of the car. At time t_k, the vehicle position is represented by the (x_k, yk) Cartesian coordinates of M in a world frame **W**. The heading angle is denoted θ_k. Let M_k and M_{k+1} be two successive positions. On the assumption that the road is perfectly planar (bump less) and as the motion is locally circular, we have (see Figure 1):

$$\delta_s = \rho \,.\, \delta_\theta, \tag{1}$$

https://doi.org/10.1017/S037346330300242X Published online by Cambridge University Press

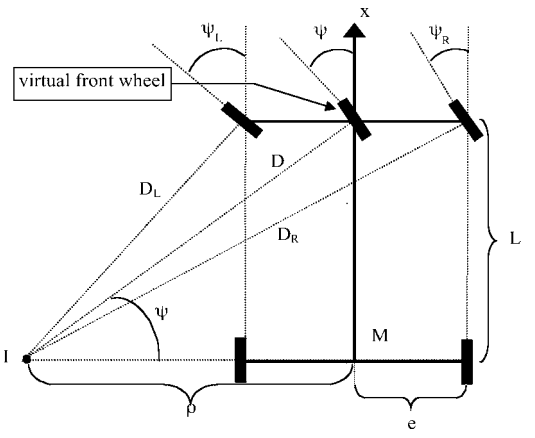

Figure 2. Ackerman model of car in a turning manoeuvre.

where δ_s is the length of the circular arc followed by M, δ_θ the elementary rotation of the mobile frame, and ρ the radius of curvature and I the instantaneous centre of rotation.

Supposing the car is moving forward, the variation in the position is expressed as:

$$\begin{cases} \Delta x = |M_k M_{k+1}| \,.\, \cos(\theta_k + \delta_\theta/2) \\ \Delta y = |M_k M_{k+1}| \,.\, \sin(\theta_k + \delta_\theta/2) \end{cases}. \tag{2}$$

From basic Euclidean geometry, one knows that $\{\delta_s \approx |M_k M_{k+1}|\}$ up to the second order. The integration process is then:

$$\begin{cases} x_{k+1} = x_k + \delta_s \,.\, \cos(\theta_k + \delta_\theta/2) \\ y_{k+1} = y_k + \delta_s \,.\, \sin(\theta_k + \delta_\theta/2) \\ \theta_{k+1} = \theta_k + \delta_\theta \end{cases}. \tag{3}$$

2.2. *Modelling the elementary displacement of a four-wheel car.* It is now necessary to estimate the input vector $\zeta = (\delta_s, \delta_\theta)^T$. Consider the four-wheel vehicle sketched in Figure 2. Let us denote e the half-track, L the wheelbase and ψ the steering angle of the virtual front wheel of the bicycle model. This angle is directly tied to the angle of the steering wheel. In order to develop an odometric model, we assume that, between two samples, the wheels do not slip and that the distances e and L are known and constant: this is a simplified view of the phenomenon occurring at the tire/ground contact zone. δ_s and δ_θ can be estimated using the steering angle ψ and the elementary distances travelled by each wheel. In the following, δ_{RL} and δ_{RR} denote the distances travelled between two samples by the rear left wheel and the rear right wheel respectively, and δ_{FL} and δ_{FR} those travelled by the front wheels.

Observation equation

The driving wheel angle ψ provides a relation between δ_s and δ_θ. Figure 2 gives:

$$\tan(\psi) = \frac{L}{\rho}. \tag{4}$$

https://doi.org/10.1017/S037346330300242X Published online by Cambridge University Press

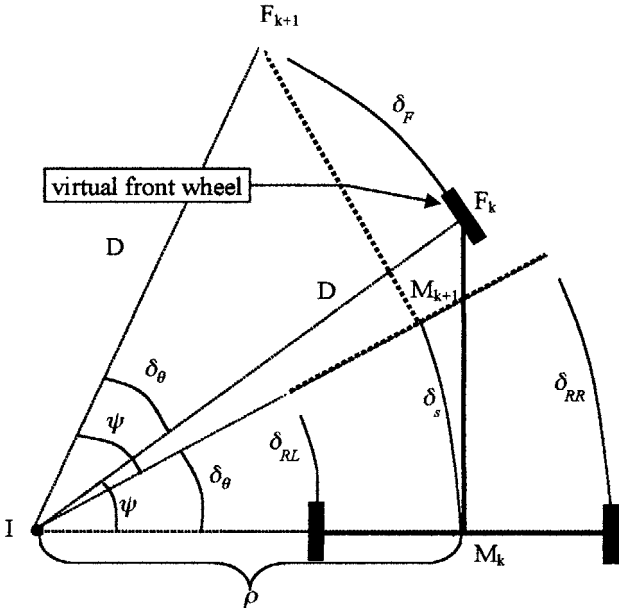

Figure 3. Elementary displacement of a car in a turning manoeuvre between time indexes k − 1 (dark) and k (light).

Equations (1) and (4) give:

$$\tan(\psi) = L\frac{\delta_\theta}{\delta_s}. \tag{5}$$

Let us consider the situation described on Fig. 3:

$$\delta_{RL} = \delta_\theta \,.\, (\rho - e) = \delta_s - e \,.\, \delta_\theta, \tag{6}$$

$$\delta_{RR} = \delta_\theta \,.\, (\rho + e) = \delta_s + e \,.\, \delta_\theta. \tag{7}$$

Commonly, in the technique called *differential odometry* (for instance, Zhao, 1997), δ_s and δ_θ are computed using just the measurements (δ_{RR}, δ_{RL}):

$$\delta_s = \frac{\delta_{RR} + \delta_{RL}}{2} \quad \delta_\theta = \frac{\delta_{RR} - \delta_{RL}}{2e}. \tag{8}$$

The measurements of the front wheels are more difficult to use because their orientation with respect to the mobile frame is not constant. In order to simplify, let consider a virtual front wheel. The length of the circular arc it follows between two samples is (see Figure 3):

$$\delta_F = D \,.\, \delta_\theta. \tag{9}$$

Now,

$$D = \frac{L}{\sin(\psi)}. \tag{10}$$

https://doi.org/10.1017/S037346330300242X Published online by Cambridge University Press

By using (4), we have:

$$D = \frac{\rho}{\cos(\psi)}. \tag{11}$$

By multiplying each side by δ_θ:

$$\delta_F \cos(\psi) = \delta_s. \tag{12}$$

The same procedure can be applied to each front wheel; it yields (ψ_L and ψ_R are shown in Figure 2):

$$\tan(\psi_L) = \frac{L}{\rho - e} \text{ and } \tan(\psi_R) = \frac{L}{\rho + e}, \tag{13}$$

ρ can be eliminated in (13) by using relation (4) to get:

$$\psi_L = \tan^{-1}\left(\frac{L\tan(\psi)}{L - e\tan(\psi)}\right) \text{ and } \psi_R = \tan^{-1}\left(\frac{L\tan(\psi)}{L + e\tan(\psi)}\right). \tag{14}$$

Finally, the adaptations of Equation (12) for each wheel are:

$$\delta_{FL} \,.\, \cos(\psi_L) = \delta_s - e \,.\, \delta_\theta, \tag{15}$$

$$\delta_{FR} \,.\, \cos(\psi_R) = \delta_s + e \,.\, \delta_\theta. \tag{16}$$

Equations (5, 6, 7, 15, 16) define a redundant and non-linear system that links the unknown quantities (δ_s, δ_θ) to the measured variables (δ_{FL}, δ_{FR}, δ_{RL}, δ_{RR}, ψ):

$$\begin{cases} \tan(\psi) & = L \,.\, \dfrac{\delta_\theta}{\delta_s} \\ \delta_{RL} & = \delta_s - e \,.\, \delta_\theta \\ \delta_{RR} & = \delta_s + e \,.\, \delta_\theta \\ \delta_{FL} \,.\, \cos(\psi_L) & = \delta_s - e \,.\, \delta_\theta \\ \delta_{FR} \,.\, \cos(\psi_R) & = \delta_s + e \,.\, \delta_\theta \end{cases}. \tag{17}$$

Defining an equivalent measurement vector (18), Equation (17) takes the usual form of an observation Equation (19).

$$z = (\tan(\psi), \delta_{RL}, \delta_{RR}, \delta_{FL} \,.\, \cos(\psi_L), \delta_{FR} \,.\, \cos(\psi_R))^{\mathrm{T}}, \tag{18}$$

$$z = h(\zeta). \tag{19}$$

2.3. *Estimation of the input vector* $\zeta = (\delta_s, \delta_\theta)^T$. Because of presence of unavoidable slippage and modelling errors, we propose to use *all* the measurements to estimate the input vector. The redundancy should reduce the effects of the unknown disturbances. Since the observation Equation (19) is non-linear, we propose to apply an Extended Kalman Filter (EKF), interpretable here as a Weighted Least Squares estimator. This technique also has the advantage of estimating the covariance of the estimation error, which will be useful for further estimation of the pose $(x, y, \theta)^T$ by EKF.

Since we use odometric models and that no acceleration or forces are supposed to be known, the variation of the state vector can be modelled by a Wiener process whose input γ_k is a zero-mean white noise with a Q_γ covariance matrix:

$$\zeta_{k+1} = \zeta_k + \gamma_k. \tag{20}$$

https://doi.org/10.1017/S037346330300242X Published online by Cambridge University Press

Since the equivalent measurements that are the components of z (Equation 18) are obtained from five different sensors, we may assume that the covariance matrix R of z is diagonal (Remembering that R is the covariance matrix of the measurement *errors*.). The EKF estimation stage can therefore be split into five independent computations, each one involving a scalar division in place of inverting a 5×5 matrix. This method improves the numerical stability and decreases the numbers of floating point operations.

Denote S_k the covariance matrix of the estimation error at time index k.
The EKF works in six steps:

Prediction stage

$$\zeta_k := \zeta_{k-1} \quad S_k := S_{k-1} + Q_r. \tag{21}$$

Estimation stages

As a first observation, Equation (17) is not defined when δ_s equals zero, it is only used when the speed of the car is high enough. Moreover, this equation being non-linear, the Jacobian matrix with respect to the state is computed at each step:

$$C_1 = \left[\frac{\delta z_1}{\delta \zeta}\right] = \left[\frac{-L\delta_\theta}{\delta_s^2}, \frac{L}{\delta_s}\right]. \tag{22}$$

Denote

$$C_2 = C_4 = [1 - e] \quad C_3 = C_5 = [1 + e]. \tag{23}$$

The following algorithm then gives the updated state and variance matrix:

for $i = 1$ to 5,

$$K_k := S_k \,.\, C_i^t \,.\, (C_i \,.\, S_k \,.\, C_i^t + R_i)^{-1} \tag{24}$$

$$\zeta_k := \zeta_k + K_k \,.\, (z_i - C_i \,.\, \zeta_k) \tag{25}$$

$$S_k := (\mathrm{I}_{22} - K_k \,.\, C_i) \,.\, S_k \tag{26}$$

end for.

Finally, each estimation of ζ_k is used in the model (3) to provide an odometric location (starting from a given position and heading). This technique is named odometric EKF in the following paragraphs.

2.4. *Sampling the odometric EKF.* Commonly, odometric models are sampled with respect to time. One should notice that they could also be sampled with respect to the distance travelled. However, the sampling rate must be such that the elementary motion is circular. In the no-slippage assumption, the motion is circular as long as the steering angle is constant. Therefore, the model should be sampled when a significant variation of the steering angle is detected during a displacement. This sampling strategy is also well adapted to the physical nature of the process: if the car is motionless, the model is not sampled and the estimation error logically does not increase. On the other hand, the position (x, y) in the model (3) is not observable from the encoder measurements (18) (Bonnifait and Garcia, 1998). One can use a GPS receiver to correct the unavoidable drift of the odometric EKF. This is nowadays an

https://doi.org/10.1017/S037346330300242X Published online by Cambridge University Press

Figure 4. The car used in the experiments.

affordable sensor, but its latency can induce unacceptable errors when the speed is high. The GPS latency is the delay between the time the measurements are made on the visible satellites and the time the position is output and received by the onboard computer. The transmission delay is unavoidable but the latency can be reduced to its minimum by using the "1PPS" signal available on the Motorola VP ONCORE used for our experiments. This signal rises each time the receiver captures the pseudo-range measurements to compute position, speed and time. Thus, we trigger the odometric EKF by using the "1PPS" signal (continuously available on the Motorola VP ONCORE).

In summary, the sampling is performed as follows:

- each time a 1PPS edge occurs,
- each time the car has travelled one metre and the steering angle has changed more than 0·5°.

The two sampling processes are asynchronous. The sampling frequency is not constant and higher than 1 Hz. It can, for example, reach several Hz while entering a roundabout.

2.5. *Tuning of the filter*. For the car used in the experiments (the Citroën Xantia Break in Figure 4), the sources of errors that affect the observation (19) are numerous. The first ones result from the limited accuracy of the ABS encoders (1·93 cm for δ_{RL}, δ_{RR}, δ_{FL}, δ_{FR}) and of the driving wheel encoder ($2.\pi/4096$ rad for ψ). Others are due to the approximate nature of the model (17) (for instance, distances e and L are not exactly constant). Since there are several uncorrelated causes of error, we suppose that inaccuracy can be globally represented by an additive zero-mean temporally uncorrelated noise. In order to tune the EKF, we have computed position errors in comparison with a post-processed DGPS. The tuning of the filter is assumed to be correct when the errors were consistent with the $\pm 3\,\sigma$ bounds.

2.6. *Results of the odometric EKF*. The experimental results presented in this section were obtained using stored data of the sensors of our experimental car. The sampling of the odometric EKF was done as presented in section 2.4. The rough measurements of the GPS receiver VP ONCORE were stored and then processed in association with a fixed receiver in order to produce what we consider to be the *true* positions of the car (Kinematic Differential GPS on L1 with the software *Jupiter*). The precision is estimated to be better than two metres while the car is moving. The

https://doi.org/10.1017/S037346330300242X Published online by Cambridge University Press

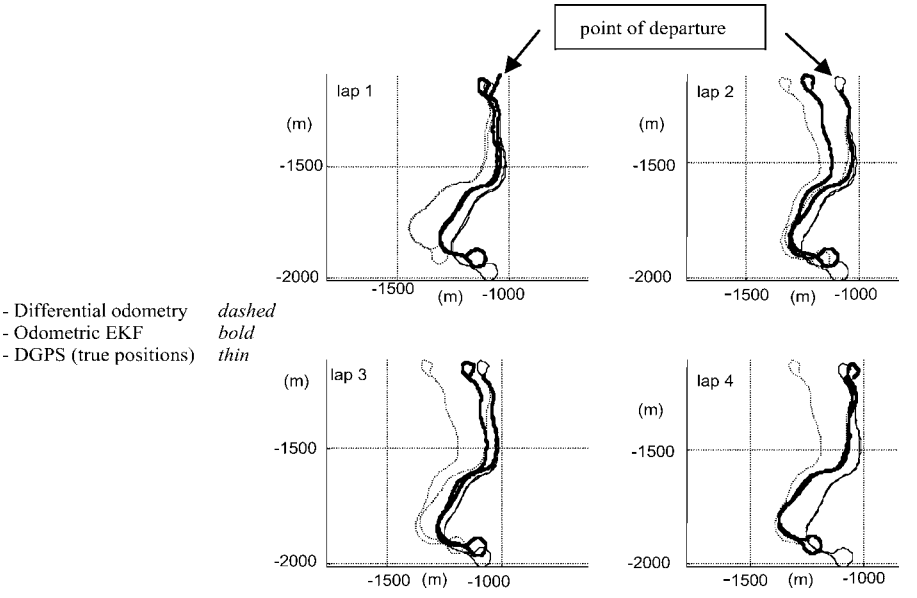

Figure 5. Top views of the experiments.

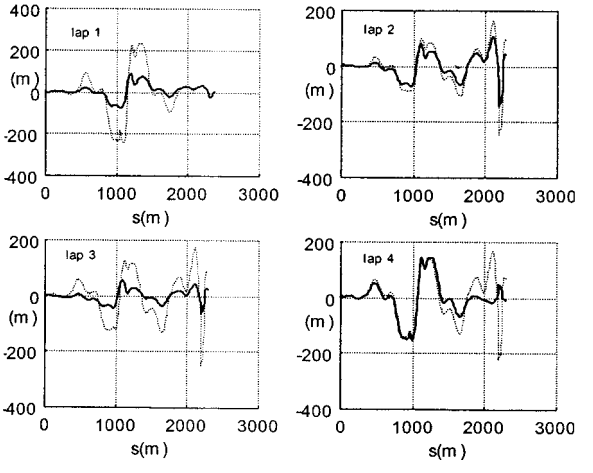

Figure 6. Longitudinal errors as functions of the distance. Odometric EKF in bold.

initial heading was computed with an error of less than 0·5°. The odometric EKF was tested on four laps, each 2·4 km long, at the maximum allowed speed of 50 km/h. The results are shown in Figure 5 (thick line) and compared with differential odometry using rear wheels only (dotted lines) and with the true trajectory (thin line). Figures 6 and 7 show longitudinal and lateral errors (with respect to the DGPS) as functions of the linear abscissa, making the benefit of the odometric EKF clearer. It can be seen from these plots that the use of all the sensors significantly increases the precision. This can be explained by the fact that, on average, the redundancy allows a better estimation. For example, slips that disturb the front wheels may not affect the

https://doi.org/10.1017/S037346330300242X Published online by Cambridge University Press

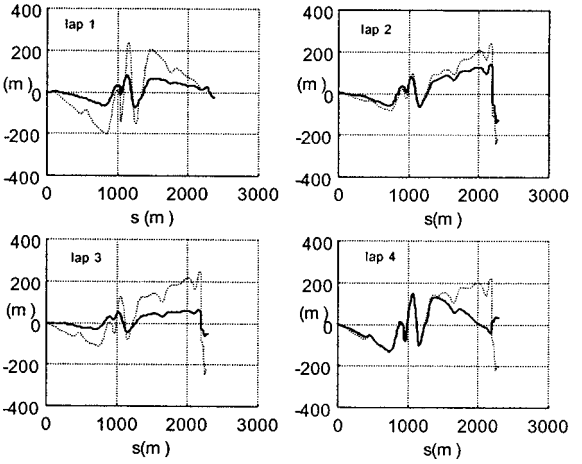

Figure 7. Lateral errors as functions of the distance. Odometric EKF in bold.

rear ones. Moreover, other experiments, not reported here, have shown that the drift of the estimation of the heading of the odometric EKF is in the same order as the one of a dead-reckoning technique using an odometer and a vibrating gyro (a British Aerospace VSG2000).

3. SENSOR FUSION OF GPS AND ODOMETRY. When a GPS position is available, a correction to the odometric estimation is performed using an Extended Kalman Filter formalism with noisy input.

3.1. *GPS latency*. As the potential applications for this method require real-time processing, the GPS receiver used in the experiments (a Motorola Oncore) was configured to reduce the output data latency to the minimum. The Oncore Receiver takes about one second to compute data from the satellite range measurements. The solution to this problem programmed in the Motorola receiver consists of computing the current position estimate using the measurements taken one second before. To compensate for the one-second computational pipeline delay, a one second propagated position is computed using the estimate of the velocity vector. In this way, the position data corresponds closely with the true receiver position. The data latency is finally reduced to the communication time on the RS232 port. (According to the manufacturer, this is less than 118 ms.)

3.2. *Architecture of the fusion process*. The odometric EKF computes an estimation of ζ and of the covariance matrix S. This data is used as the input for a second EKF estimating x, y, θ. The measurements (x, y) of the GPS (in a local ground frame) are used as the observations. This architecture, depicted in Figure 8, can be seen as a "loosely coupled fusion system".

3.3. *Heading observability*. The heading, θ, is not directly measured since the GPS is used as a position sensor. Nevertheless, by studying the state observability of the non-linear system (Bonnifait and Garcia, 1998), it is easy to verify that the observability condition is verified when the speed of the car is non-zero. In order to assess what happens in this case, let consider a car when it stops: the measurement δ_θ becomes zero without any noise (no signal comes from the ABS encoders) and the

https://doi.org/10.1017/S037346330300242X Published online by Cambridge University Press

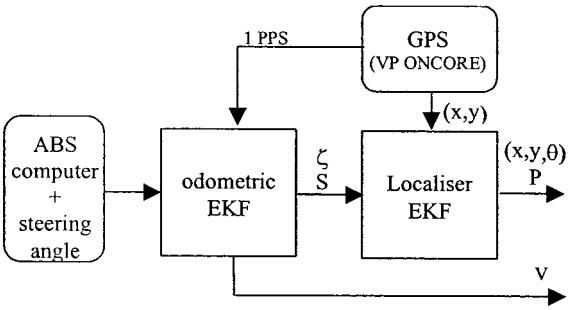

Figure 8. Architecture of the localization system.

odometric prediction of the heading does not change. This is interesting when compared with a dead reckoning system using a gyro that will suffer from drifting under the same conditions. When the vehicle moves again, the localizer will start with a non-deteriorated heading estimate.

3.4. *Tuning the filter*. The position errors measured by GPS (with the SA degradation off) are temporally correlated. We have estimated a first order Auto-Regressive (AR) model (Cooper and Durrant-Whyte, 1994) of the noise. The time-constant of this AR model is approximately 2 hours. This value exceeds the time-constant desired for the filter by several degrees of magnitude. It is thus not good to define an augmented state that incorporates this AR model. One practical solution to take into account the correlation of the noise is to increase the variance of the observations. If this were not done, the filter would yield erroneous estimations that were too confident. In the experiments presented in this paper, we have estimated the variances Rx and Ry of the observations using a 3-day long data recording.

$$Rx = 1{\cdot}22^2\text{m}^2 \quad \text{and} \quad Ry = 2{\cdot}75^2\text{m}^2. \tag{27}$$

Then, we have used a 5 ratio for the augmentation.

The GPS data changes with the number of visible satellites and their geometrical configuration (for example, characterized by the Position Dilution Of Precision (PDOP) coefficient). Some receivers provide estimates of the latitude and longitude variances that follow the satellite changes, but not the Motorola Oncore (it performs a least squares estimation). In Thrapp, Westbrook and Subramanian, 2001, the authors handle the non-stationarity in the variance of the GPS measurements using, first, distinct covariance matrices for each number of satellites and then, secondly, an average value of the innovation error of the Kalman filter. This method is well adapted if the receiver is configured to use all the satellites that it is tracking. Otherwise, the receiver uses the best four satellites as defined by a PDOP selection. In this case, a change in the number of satellites is not an indicator of a GPS data change. Another approach, and the technique used in our experiments to take into account this non-stationarity, is to inflate the state covariance matrix each time a PDOP changes significantly.

3.5. *Results*. The global localizer was tested on the four laps of the experiment described in section 2.6, a total distance of 9·6 km. The first rough GPS measurement was used to initialize the two first components of the state of the Kalman filter and the initial estimate of the heading was arbitrarily set to zero. Errors were computed by post-processed DGPS.

https://doi.org/10.1017/S037346330300242X Published online by Cambridge University Press

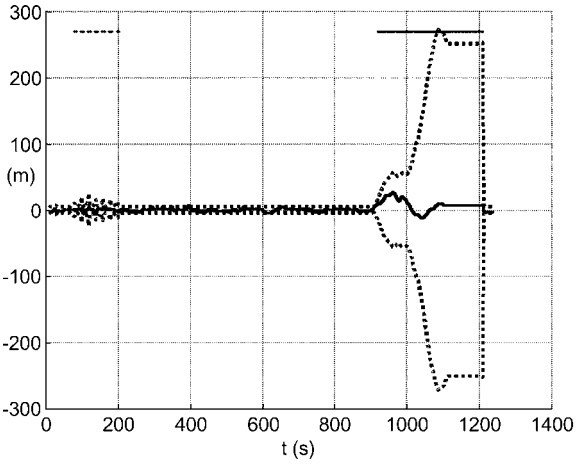

Figure 9. X error and 3σ estimated bounds.

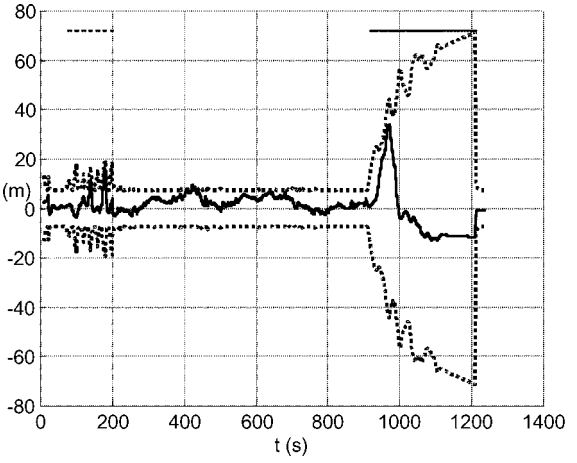

Figure 10. Y error and 3σ estimated bounds.

Three features were tested in this experiment:

- The normal operation with all measurements available.
- Seven small GPS obscurations of ten seconds (for $70 < t < 210$ s), similar to the ones observed in town circuits.
- A large obscuration of 5 minutes (for $900 < t < 1200$ s) to test the robustness of the error computation.

Figures 9, 10, 11 and 12 present the results (the dotted lines are the 3σ estimated bounds). Despite the computation with a linearized model, the large obscuration of GPS signals shows that the errors have been estimated well since the confidence bounds are consistent with the errors (9 and 10). Figures 11 and 12 focus on interesting parts of Figure 9. In Figure 11, it can be seen that each time an obscuration of GPS signals occurs, the error is consistent with the estimated confidence. This

https://doi.org/10.1017/S037346330300242X Published online by Cambridge University Press

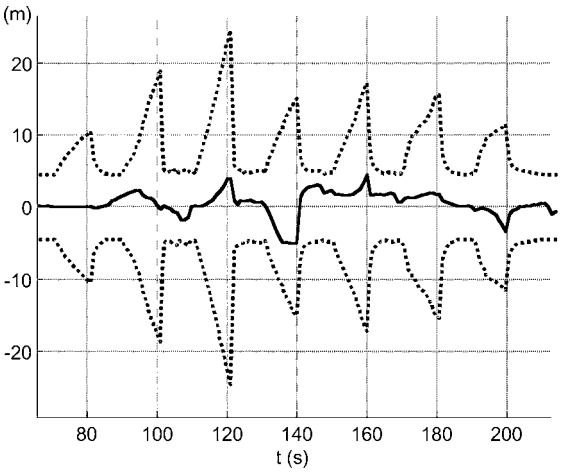

Figure 11. X error during the small GPS obscurations (zoom of Fig. 9).

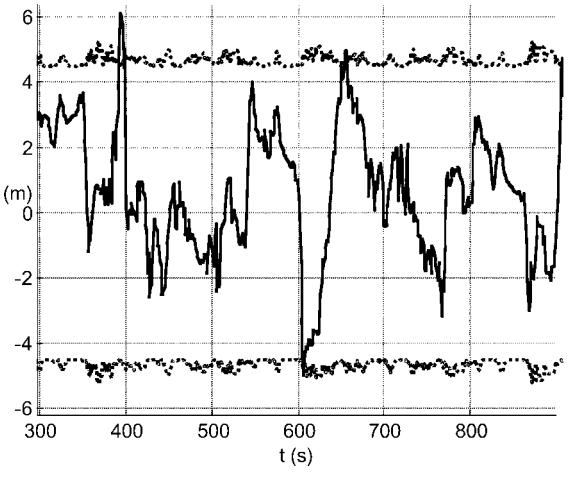

Figure 12. X error when the GPS is locked on (zoom of Fig. 9).

realistic situation gives an idea of the actual precision (a few metres) of the localization. Figure 12 indicates that the filter is well tuned since the estimated 3-standard deviation is consistent with the error. As expected, the position error is mainly from the GPS and therefore is not white.

4. CONCLUSION. This work has presented the development of a localization system and its real world experimentation. It is a very cheap localizer, since it uses a normal GPS receiver and the ABS sensors available on most modern cars. Due to an adequate sampling rate, the proposed odometric method is computed when necessary and in a way well adapted to a GPS correction. The experiments have proved that the use of all the four ABS sensors on a vehicle increases the precision of the positioning system in comparison with the use of only the two associated with the rear wheels. This dead-reckoning technique is sufficient to maintain

https://doi.org/10.1017/S037346330300242X Published online by Cambridge University Press

a precise estimation of the position during small GPS obscurations. During large obscurations, we think it will produce an efficient estimation of the local trajectory, which should be useful for the map-matching process with a precise digital map. Our future work will centre on the study of an automatic calibration of wheel circumference. We have already found that the circumference changes with tyre wear but it is not very sensitive to the variation of tyre pressure.

REFERENCES

Abbott, E. and Powel, D. (1999). Land-Vehicle Navigation using GPS. *Proceedings of the IEEE*. Vol. **87**, No. 1.

Barshan, B. and Durrant-Whyte, H. F. (1995). Inertial navigation systems for mobile robots. *IEEE Transactions on Robotics and Automation*. Vol. **11**, No. 3.

Bétaille, D. and Bonnifait, Ph. (2002). Vehicles Modelling and Multi-Sensor Smoothing Techniques for Post-Processed Vehicles Localisation. *Institute Of Navigation GPS*. Portland, Oregon. September.

Bonnifait, Ph. and Garcia, G. (1998). Design and Experimental Validation of an Odometric and Goniometric Localization System for Outdoor Robot Vehicles. *IEEE Transactions on Robotics and Automation*. Vol. **14**, No. 4.

Chung, H., Ojeda, L. and Borenstein, J. (2001). Sensor fusion for Mobile Robot Dead-reckoning With a Precision-calibrated Fibre Optic Gyroscope. *International Conference on Robotics and Automation*. Seoul, May 21–26.

Cooper, S. and Durrant-Whyte, H. (1994). A Kalman Filter Model for GPS Navigation of Land Vehicles. *IROS*. Sept. Munich. 157–163.

Guivant, J., Nebot, E. and Baiker, S. (2000). High accuracy Navigation Using Laser Range Sensors in outdoors Applications. *International Conference on Robotics and Automation*. San Francisco.

Julier, S. and Durrant-Whyte, H. (1995). Process Models For The High-Speed Navigation of Road Vehicles. *International Conference on Robotics and Automation*.

Kochem, M., Wagner, N., Hamann, C.-D. and Isermann, R. (2002). Data fusion for precise dead reckoning of passenger cars. *IFAC 15th Triennial World Congress*, Barcelona, July.

Thrapp, R., Westbrook, C. and Subramanian, D. (2001). Robust localization algorithms for an autonomous campus tour guide. *International Conference on Robotics and Automation*. Seoul, May 21–26.

Zhao, Y. (1997). *Vehicle Location and Navigation Systems*. Artech House.

Zhao, Y. (2000). Mobile Phone Location Determination and Its Impact on Intelligent Transportation Systems. *IEEE Transactions On Intelligent Transportation Systems*. Vol. **1**, No. 1, March.